12. Visscher, E. H. *et al.* Broadband single-electron tunneling transistor. *Appl. Phys. Lett.* **68,** 2014–2016 (1996).
13. Visscher, E. *Technology and Applications of Single-Electron Tunneling Devices*. Ph.D thesis, Delft Univ. Technol. (1996).
14. Lu, W., Ji, Z. Q., Pfeiffer, L., West, K. W. & Rimberg, A. J. Real-time detection of electron tunnelling in a quantum dot. *Nature* **423,** 422–425 (2003).
15. Fujisawa, T., Hayashi, T., Hirayama, Y., Cheong, H. D. & Jeong, Y. H. Electron counting of single-electron tunneling current. *Appl. Phys. Lett.* **84,** 2343–2345 (2004).
16. Blanter, Ya. M. & Büttiker, M. Shot noise in mesoscopic conductors. *Phys. Rep.* **336,** 1–166 (2000).
17. Cleland, A. N., Schmidt, J. M. & Clarke, J. Charge fluctuations in small-capacitance junctions. *Phys. Rev. Lett.* **64,** 1565–1568 (1990).
18. Kuzmin, L. S., Nazarov, Yu. V., Haviland, D. B., Delsing, P. & Claeson, T. Coulomb blockade and incoherent tunneling of Cooper pairs in ultrasmall junctions affected by strong quantum fluctuations. *Phys. Rev. Lett.* **67,** 1161–1164 (1991).
19. Delsing, P., Likharev, K. K., Kuzmin, L. S. & Claeson, T. Effect of high-frequency electrodynamic environment on the single-electron tunneling in ultrasmall junctions. *Phys. Rev. Lett.* **63,** 1180–1183 (1989).
20. Korotkov, A. N. Analytical calculation of single-electron oscillations in one-dimensional arrays of tunnel junctions. *Phys. Rev. B* **50,** 17674–17677 (1994).
21. Likharev, K. K. Single-electron transistors: Electrostatic analogs of the dc-squids. *IEEE Trans. Magn.* **23,** 1142–1145 (1987).
22. Fulton, T. A. & Dolan, G. J. Observation of single-electron charging effects in small tunnel junctions. *Phys. Rev. Lett.* **59,** 109–112 (1987).
23. Schoelkopf, R. J., Wahlgren, P., Kozhevnikov, A. A., Delsing, P. & Prober, D. E. The radio-frequency single-electron transistor (RF-SET): A fast and ultrasensitive electrometer. *Science* **280,** 1238–1242 (1998).
24. Pashkin, Y. A., Nakamura, Y. & Tsai, J. S. Metallic resistively coupled single-electron transistor. *Appl. Phys. Lett.* **74,** 132–134 (1999).
25. Korotkov, A. N. Theoretical analysis of the resistively coupled single-electron transistor. *Appl. Phys. Lett.* **72,** 3226–3228 (1998).
26. Delsing, P., Claeson, T., Kazacha, G. S., Kuzmin, L. S. & Likharev, K. K. 1-D array implementation of the resistively-coupled single-electron transistor. *IEEE Trans. Magn.* **27,** 2581–2584 (1991).
27. Bakhvalov, N. S., Kazacha, G. S., Likharev, K. K. & Serdyukova, S. I. Single-electron solitons in one-dimensional tunnel structures. *Sov. Phys. JETP* **68,** 581–587 (1989).
28. Dolan, G. J. Offset masks for lift-off photoprocessing. *Appl. Phys. Lett.* **31,** 337–339 (1977).
29. Levitov, L. S., Lee, H. & Lesovik, G. B. Electron counting statistics and coherent states of electric current. *J. Math. Phys.* **37,** 4845–4866 (1996).
30. Middleton, A. A. & Wingreen, N. S. Collective transport in arrays of small metallic dots. *Phys. Rev. Lett.* **71,** 3198–3201 (1993).
31. Kaplan, D. M., Sverdlov, V. A. & Likharev, K. K. Coulomb gap, Coulomb blockade, and dynamic activation energy in frustrated single-electron arrays. *Phys. Rev. B* **68,** 45321 (2003).

Acknowledgements We thank C. Kristoffersson, S. Pedersen and P. Wahlgren for assistance in the early stages of this work, K. Bladh, D. Gunnarsson, S. Kafanov and M. Taslakov for technical assistance, and T. Claeson, H. Nilsson, K-E. Rydler, G. Wendin, C. Wilson and A. Zorin for discussions. The work was supported by the Swedish SSF and VR, by the EU research project COUNT and by the Wallenberg foundation.

Competing interests statement The authors declare that they have no competing financial interests.

Correspondence and requests for materials should be addressed to J.B. (jonas.bylander@mc2.chalmers.se).

Relaxor ferroelectricity and colossal magnetocapacitive coupling in ferromagnetic $CdCr_2S_4$

J. Hemberger[1], P. Lunkenheimer[1], R. Fichtl[1], H.-A. Krug von Nidda[1], V. Tsurkan[1,2] & A. Loidl[1]

[1]Experimental Physics V, Centre for Electronic Correlations and Magnetism, University of Augsburg, 86159 Augsburg, Germany
[2]Institute for Applied Physics, Academy of Sciences of Moldova, MD-2028, Chisinau, Moldova

Materials in which magnetic and electric order coexist—termed 'multiferroics' or 'magnetoelectrics'—have recently become the focus of much research[1–4]. In particular, the simultaneous occurrence of ferromagnetism and ferroelectricity, combined with an intimate coupling of magnetization and polarization via magnetocapacitive effects, holds promise for new generations of electronic devices. Here we present measurements on a simple cubic spinel compound with unusual, and potentially useful, magnetic and electric properties: it shows ferromagnetic order coexisting with relaxor ferroelectricity (a ferroelectric cluster state with a smeared-out phase transition), both having sizable ordering temperatures and moments. Close to the ferromagnetic ordering temperature, the magnetocapacitive coupling (characterized by a variation of the dielectric constant in an external magnetic field) reaches colossal values, approaching 500 per cent. We attribute the relaxor properties to geometric frustration, which is well known for magnetic moments but here is found to impede long-range order of the structural degrees of freedom that drive the formation of the ferroelectric state.

Preparation of a material in which ferroelectricity and ferromagnetism coexist would be a milestone for modern electronics and functionalized materials. The most appealing applications of such a material are new types of storage media using both magnetic and electric polarization, and the possibility of electrically reading/writing magnetic memory devices (and vice versa). However, it is clear now that ferroelectric ferromagnets are rare[5,6] and mostly exhibit rather weak ferromagnetism. Spinel compounds are an important class of materials, and their electronic properties have been the focus of research since the work of Verwey on magnetite[7]. Recent reports of geometrical frustration of the spin and orbital degrees of freedom in sulpho-spinels[8], and the observation of an orbital-glass state[9] in these compounds, demonstrate the rich and complex physics that is characteristic of this system. Here we report another interesting experimental observation in a spinel system: relaxor ferroelectricity in ferromagnetic $CdCr_2S_4$ and the occurrence of colossal magnetocapacitive effects.

$CdCr_2S_4$ crystallizes in the normal cubic spinel structure (space group $Fd3m$, lattice constant $a = 1.024$ nm), with Cr^{3+} octahedrally surrounded by sulphur ions, yielding a half-filled lower t_{2g} triplet with spin $S = 3/2$. Ferromagnetism in $CdCr_2S_4$ is well known[10], but early experimental observations of a number of unusual features seem to have been overlooked: for example, reports of an anomalous expansion coefficient at low temperatures[11,12], an unexpected concomitant broadening of the diffraction lines[11], a strong blue shift of the absorption edge on passing the ferromagnetic phase transition[13], the observation of anomalously large phonon shifts and damping effects close to the magnetic transition temperature T_c (ref. 14), and the observation of large magnetoresistance effects[15].

Figure 1a shows the inverse magnetic susceptibility χ^{-1} and the low-temperature (low-T) magnetization M. The straight line indicates a fit to the paramagnetic susceptibility, which results in a Curie–Weiss temperature of 155 K and a paramagnetic moment of 3.88 μ_B, close to the theoretically expected value of 3.87 μ_B per Cr^{3+}. The deviations when approaching T_c arise from ferromagnetic fluctuations. $M(T)$ strongly increases at T_c, the further increase just below T_c being interrupted by demagnetization effects. The inset in Fig. 1a shows the ferromagnetic hysteresis, revealing soft-magnetic behaviour and a saturation magnetization of 3 μ_B per Cr^{3+}. Hence, $CdCr_2S_4$ behaves like a typical soft ferromagnet.

Figure 1b shows the temperature dependence of the dielectric constant ε', measured at 9.5 Hz (right scale). $\varepsilon'(T)$ exhibits a steep rise below T_c, obviously driven by the onset of ferromagnetic order. Strong magnetoelectric coupling effects must be responsible for this behaviour. At lower temperatures, $\varepsilon'(T)$ decreases again, leading to a maximum reminiscent of ferroelectric behaviour. However, its rather large width and the only moderately high maximum values of $\varepsilon' \approx 100$ indicate a transition into a polar state of diffusive character. Indeed, a finite polarization, a direct proof of ferroelectricity, arises well below T_c (Fig. 1b, left scale). Final evidence is provided in Fig. 1c, which shows a polarization cycle (using electric fields up to 400 kV m^{-1}) exhibiting a clear ferroelectric hysteresis. But the relatively slim loop indicates non-canonical ferroelectric behaviour[16].

Evidence for the actual character of this ferroelectric state is revealed by the temperature dependence of ε', shown in Fig. 2a for a series of measuring frequencies. A very broad peak appears between 150 and 250 K, shifting to lower temperatures and increasing in amplitude with decreasing frequency. It exhibits the characteristic behaviour of a relaxor ferroelectric, the typical strong dispersion effects often being ascribed to the freezing-in of ferroelectric clusters[16,17]. In contrast to conventional ferroelectrics, relaxor ferroelectrics are characterized by a diffuse phase transition (extending over a finite temperature range), by strong relaxational dispersion effects in dielectric constant and loss, and by a macroscopic polarization showing up only well below the transition temperature[16–18]. Most relaxor ferroelectrics known so far are perovskite-related materials where long-range polar order is suppressed by substitutional disorder[17]. However, the relaxor properties in $CdCr_2S_4$ occur in a pure compound without any disorder. By comparison to measurements with silver-paint contacts (not shown), the increase of ε' at temperatures above those at which the peak occurs is found to be due to contact effects[19], whereas the peak itself is clearly an intrinsic property of $CdCr_2S_4$. The high-temperature flank of the relaxor peaks can be roughly described by a Curie–Weiss law with a characteristic temperature of 135 K (dashed line in Fig. 2a). In relaxors, deviations from a Curie–Weiss law are often observed; but this law gives a rough estimate of a quasistatic freezing temperature. Notably, significant spontaneous polarization sets in only well below 135 K, a behaviour often found in relaxor ferroelectrics[17].

Further evidence for typical relaxor behaviour arises from the frequency (ν) dependence of the dielectric loss ε''. The inset of Fig. 2a shows $\varepsilon''(\nu)$ for a series of temperatures, obtained after subtraction of a conductivity contribution. Broad peak maxima are revealed, typical of relaxational behaviour. The peak frequency decreases when the temperature is lowered, indicating the freezing-in of polar moments. In $CdCr_2S_4$, the half-width of the loss peak at 151 K amounts to nearly three decades in frequency, significantly broader than the 1.14 decades expected for a Debye relaxation, indicating a broad distribution of relaxation times. However, in most canonical relaxors even broader distributions are found[17,18], and we cannot exclude the possibility that contributions from hopping charge carriers (for example, small polarons trapped in defects[20]) play a role in the appearance of the observed relaxation feature.

A second relaxation-derived dispersion with a concomitant strong increase of ε' appears at temperatures below the onset of ferromagnetic order (Fig. 2a). A double peak appearing at low frequencies becomes increasingly suppressed at higher frequencies. This can be explained by assuming that the polar moments, which at about 100 K are frozen-in at the timescale of the experiment, speed up again below T_c. The increasing ferromagnetic correlations accelerate the mean polar relaxation rates. This leads to a remelting of the frozen-in relaxor state at $T < T_c$, resulting in strongly enhanced dielectric constants. Only when the temperature is further lowered (below about 20 K) does temperature finally 'win', and ε' becomes reduced owing to a complete freezing-in of the polar dynamics. Most probably, exchangestriction (volume changes arising from the magnetic exchange energy) softens the lattice, reduces the energy barriers against dipolar reorientation and enhances the mean relaxation rates. Exchangestriction was also used to explain the enormous blue shift in $CdCr_2S_4$ (ref. 21). On the other hand, a contribution from hopping-type charge transport to the anomaly at T_c by way of a variation of the a.c. conductivity, also affecting ε', cannot be excluded, especially as it is well known that $CdCr_2S_4$ exhibits sizable magnetoresistance effects[15]. In any case, overall the magnetocapacitive coupling in $CdCr_2S_4$ is different to all mechanisms observed so far and purely dynamic in origin.

Figure 2b demonstrates that the magnetocapacitive coupling is indeed extremely strong and can be termed colossal. It shows the temperature dependence of the dielectric constant at 9.5 Hz and 17 kHz as measured in zero magnetic field and in a field of 5 T. The relaxation dynamics at $T > T_c$ remain essentially unaffected by the field. However, strong magnetocapacitive effects are observed close to T_c. The magnetocapacitance—as derived from the difference of the dielectric constant in zero and non-zero fields—is shown in the inset of Fig. 2b. At low measuring frequencies, the maximum effects occurring close to T_c reach 450% at 9.5 Hz. For possible applications of this phenomenon, some hurdles certainly have to be overcome: for example, by doping or searching for related multiferroic spinel systems with higher transition temperatures.

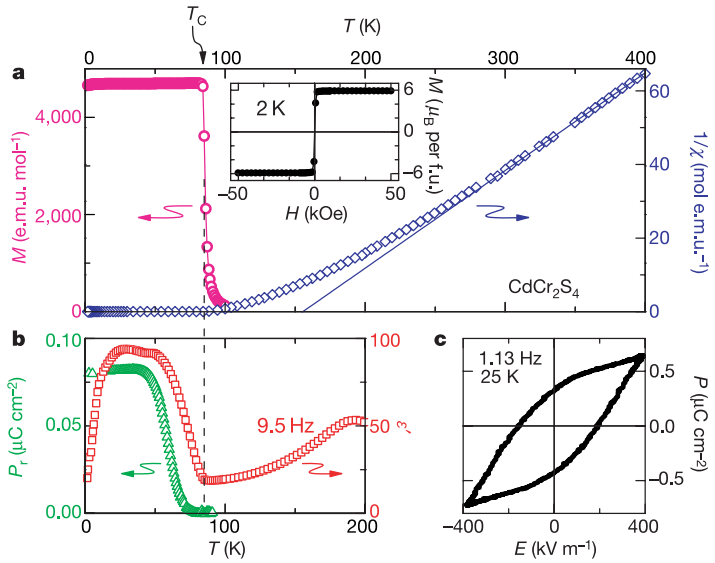

Figure 1 Magnetic and dielectric characterization of $CdCr_2S_4$. **a**, Right scale: inverse magnetic susceptibility versus temperature measured at 100 Oe. The solid line indicates a fit ($T > 300$ K) using a Curie–Weiss law, with a Curie–Weiss temperature of 155 K. Left scale: magnetization versus temperature measured at 100 Oe. Inset: ferromagnetic hysteresis at 2 K, indicating a saturated moment of 6 μ_B per formula unit (f.u.). **b**, Right scale: dielectric constant versus temperature measured at a frequency of 9.5 Hz. Left scale: thermo-remanent polarization versus temperature measured after cooling in an electric field of 50 kV m^{-1}. **c**, Polarization versus electric field, showing a ferroelectric hysteresis.

Finally, Fig. 3 shows the thermo-remanent polarization (P) for various magnetic fields, demonstrating a strong coupling of both quantities. Increasing external magnetic fields suppress the polar state, in marked contrast to the findings in other magnetocapacitive materials[1–3]. This is fully consistent with our assumption that the onset of ferromagnetic order enhances the reorientational mobility of the polar entities. Increasing magnetic fields drive the system towards ferromagnetism, and thus the macroscopic polarization breaks down at lower temperatures for higher fields (Fig. 3). The polarization shift increases with magnetic field (inset of Fig. 3), showing the strong competition between ferroelectricity and ferromagnetism. The magnetic-field dependence shown in Figs 2b and 3 was measured with the electric field perpendicular to the magnetic field; measurements with the electric field parallel to the magnetic field led to identical results.

Two more questions remain to be resolved: what is the nature of the ordered dipolar moment in $CdCr_2S_4$, and how could relaxor ferroelectricity occur without disorder-derived frustration? It is clear that the polar ordering must be displacive in nature, driven by soft-mode behaviour as in ferroelectric perovskites. This notion is consistent with the above-mentioned structural softening deduced in ref. 11. Indeed, the observation of polar displacements of the octahedrally coordinated ions has been reported for a number of spinels[22]. Guided by these results, we suggest that ferroelectricity in $CdCr_2S_4$ results from an off-centre position of the Cr^{3+} ions. It may well be that spinel compounds will turn out to be a new class of semiconducting ferroelectrics.

In relaxor ferroelectrics, the freezing of polar moments is driven by frustrated interactions related to disorder. For magnetic systems, frustration can also arise in ordered solids from geometrical constraints alone[23]. Ising spins with nearest-neighbour antiferromagnetic interactions on a triangular lattice are a standard example. The possibility that geometric frustration might also exist in non-magnetic systems has been suggested[24], exemplified by ZrW_2O_8 revealing negative thermal expansion[25]. This effect has been explained with a concept of frustrated soft-mode behaviour[26]. $CdCr_2S_4$ also shows negative thermal expansion, and reveals a strong broadening of diffraction lines below 120 K (refs 11,12). The broadening of diffraction lines on cooling provides clear evidence for the loss of true long-range order, and indicates that local order may differ substantially from global symmetry. Similar effects have been observed[27] in the orientational glass KBr:KCN. In orientational glasses[28], disorder-derived frustration drives the glassy freezing. In contrast, the suggested polar freezing in $CdCr_2S_4$ could be governed by geometrical constraints.

The most interesting aspects of the behaviour of $CdCr_2S_4$ are the coexistence of ferromagnetism and proper ferroelectricity (with reasonable ordering temperatures and sizable saturated moments), colossal magnetocapacitive effects, and strong coupling of ferroelectric polarization to external magnetic fields. Compared to recent reports on other multiferroics[1–4], this spinel system is unique. The perovskite-derived manganites treated in refs 1–3 are improper ferroelectrics with polar order induced by modulated spin structures, accompanied by lattice modulations. In contrast, the hexagonal manganite of ref. 4 is a proper ferroelectric with high ordering temperature ($T_c = 875$ K) and much lower antiferromagnetic ordering ($T_N = 75$ K). Ferromagnetism is induced by applied electric fields. In $CdCr_2S_4$, ferromagnetism and ferroelectricity to first order develop independently, driven by electronic superexchange and soft-mode behaviour, respectively. Both phenomena are linked to the Cr^{3+} ions and strongly compete, yielding colossal magnetoelectric effects. In $CdCr_2S_4$, magnetization and polarization, as well as dipolar and magnetic susceptibilities, are compatible with a global cubic symmetry. All quantities are independent of the

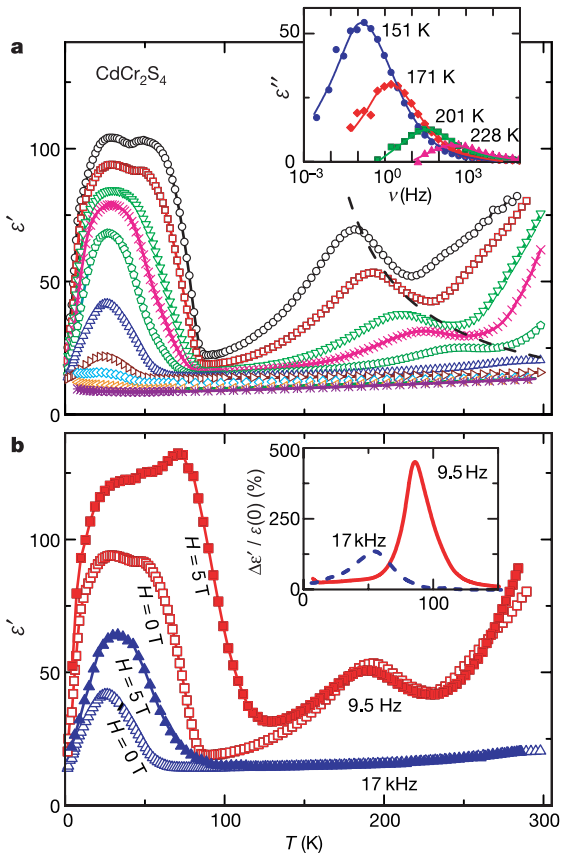

Figure 2 Magnetocapacitive behaviour of $CdCr_2S_4$. **a**, Temperature dependence of ε' at various frequencies (from top to bottom: 3 Hz, 9.5 Hz, 53 Hz, 170 Hz, 950 Hz, 17 kHz, 950 kHz, 12 MHz, 83 MHz, 3 GHz). The dashed line indicates the static dielectric susceptibility following a Curie–Weiss-like law with a characteristic temperature of 135 K. The inset shows $\varepsilon''(\nu)$ for various temperatures above 150 K (lines are to guide the eye). **b**, Dielectric constant versus temperature at 9.5 Hz and 17 kHz, measured at zero field and in an external magnetic field of 5 T, directed perpendicular to the electric field. The inset provides a measure of the magnetocapacitive effects, with $\Delta\varepsilon' = \varepsilon'(5\text{T}) - \varepsilon'(0\text{T})$, for the two frequencies shown in the main panel.

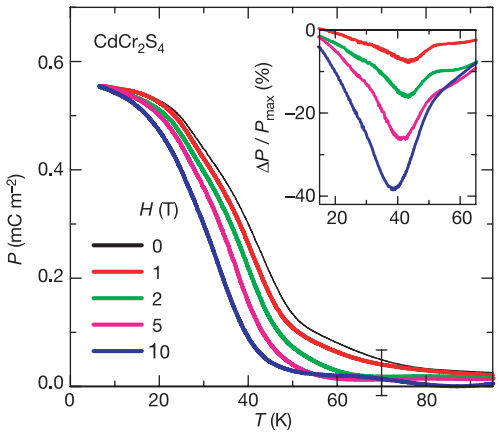

Figure 3 Thermo-remanent polarization versus temperature. Measurements were made after cooling the sample in an electric field of 150 kV m^{-1} in various external magnetic fields, directed perpendicular to the electric field. The error bar indicates an 80% confidence error caused by conductivity contributions. The inset shows the magnetic-field-dependent variation of the polarization, $\Delta P = P(H) - P(0\text{T})$, normalized to the maximum polarization of about 0.55 mC m^{-2}. Colour coding as in main panel; x axis shows temperature in K.

direction of the magnetic field with respect to the electric field, indicating that $CdCr_2S_4$ belongs to a new class of multiferroics. Despite these differences, frustration seems to play a fundamental role in all these multiferroic compounds: it is frustration of the electronic degrees of freedom in the manganites, and geometrical frustration of the lattice degrees of freedom in the spinel. □

Methods

Single crystals of $CdCr_2S_4$ were grown by chemical transport reaction, using chlorine as the transport agent. The starting material was the ternary compound obtained by standard ceramic techniques. The single crystals were routinely characterized by powder and single-crystal X-ray diffraction, and by wavelength sensitive electron-probe microanalysis. We found an almost ideal stoichiometry, and we can exclude any site inversion between the cations. To check for the robustness of the results, we performed measurements on several crystals from different batches. All samples revealed ferromagnetic and ferroelectric ordering temperatures well within the experimental uncertainties. Magnetic susceptibility and magnetization were measured using a commercial SQUID. For the dielectric measurements of the present work, sputtered gold contacts were applied to the plate-like samples, forming a parallel-plate capacitor. To check for possible contributions from electrode polarization, the same sample was also measured with silver-paint contacts. The dielectric constant and loss were measured over a broad frequency range of nine decades ($3\,Hz < \nu < 3\,GHz$). A frequency-response analyser (Novocontrol α-analyser) was used for frequencies $\nu < 1\,MHz$, and a reflectometric technique using an impedance analyser (Agilent E4291A) for $\nu > 1\,MHz$ (ref. 29). The temperature-dependent polarization was determined via the pyro charge measured with an electrometer (Keithley 617). The same device was used as impedance transformer within a Sawyer-Tower circuit, read out by a two-channel digital oscilloscope (Tektronik TDS210) and stimulated via a high-voltage amplifier (Trek 609). For cooling to temperatures down to 1.4 K, a conventional ^{4}He bath-cryostat (Cryovac Konti-IT) was used; additional magnetic-field-dependent measurements up to 10 T were performed in an Oxford cryomagnet. The magnetic anisotropy was checked by angular-dependent SQUID and electron-spin-resonance measurements. We found almost isotropic behaviour in the paramagnetic phase, and a slight cubic anisotropy in the magnetically ordered phase. All dielectric measurements were performed with $\mathbf{E}\|\mathbf{H}$ and $\mathbf{E}\perp\mathbf{H}$, and we also measured along different crystallographic directions, revealing identical results within experimental resolution.

Received 19 November; accepted 23 December 2004; doi:10.1038/nature03348.

1. Kimura, T. *et al.* Magnetic control of ferroelectric polarization. *Nature* **426,** 55–58 (2003).
2. Goto, T., Kimura, T., Lawes, G., Ramirez, A. P. & Tokura, Y. Ferroelectricity and giant magnetocapacitance in perovskite rare-earth manganites. *Phys. Rev. Lett.* **92,** 257201 (2004).
3. Hur, N. *et al.* Electric polarization in a multiferroic material induced by magnetic fields. *Nature* **429,** 392–395 (2004).
4. Lottermoser, Th. *et al.* Magnetic phase control by an electric field. *Nature* **430,** 541–544 (2004).
5. Hill, N. A. Why are there so few magnetic ferroelectrics? *J. Chem. Phys. B* **104,** 6694–6709 (2000).
6. Smolenskii, G. A. & Chupis, I. E. Ferroelectromagnets. *Sov. Phys. Usp.* **25,** 475–493 (1983).
7. Verwey, J. E. W. Electronic conduction of magnetite (Fe_3O_4) and its transition point at low temperature. *Nature* **144,** 327–328 (1939).
8. Fritsch, V. *et al.* Spin and orbital frustration in $MnSc_2S_4$ and $FeSc_2S_4$. *Phys. Rev. Lett.* **92,** 116401 (2004).
9. Fichtl, R., Tsurkan, V., Lunkenheimer, P., Hemberger, J., Fritsch, V., Krug von Nidda, H.-A., Scheidt, E.-W. & Loidl, A. Orbital freezing and orbital glass state in $FeCr_2S_4$. *Phys. Rev. Lett.* **94,** 027601 (2005).
10. Baltzer, P. K., Lehmann, H. W. & Robbins, M. Insulating ferromagnetic spinels. *Phys. Rev. Lett.* **15,** 493–495 (1965).
11. Göbel, H. Local lattice distortions in chromium chalcogenide spinels at low temperatures. *J. Magn. Magn. Mater.* **3,** 143–146 (1976).
12. Martin, G. W., Kellog, A. T., White, R. L. & White, R. M. Exchangestriction in $CdCr_2S_4$ and $CdCr_2Se_4$. *J. Appl. Phys.* **40,** 1015–1016 (1969).
13. Harbeke, G. & Pinch, H. Magnetoabsorption in single-crystal semiconducting ferromagnetic spinels. *Phys. Rev. Lett.* **17,** 1090–1092 (1966).
14. Wakamura, K. & Arai, T. Effect of magnetic ordering on phonon parameters for infrared active modes in ferromagnetic spinel $CdCr_2S_4$. *J. Appl. Phys.* **63,** 5824–5829 (1988).
15. Lehmann, H. W. & Robbins, M. Electrical transport properties of the insulating ferromagnetic spinels $CdCr_2S_4$ and $CdCr_2Se_4$. *J. Appl. Phys.* **37,** 1389–1390 (1966).
16. Samara, G. A. The relaxation properties of compositionally disordered ABO_3 perovskites. *J. Phys. Condens. Matter* **15,** R367–R411 (2003).
17. Cross, L. E. Relaxor ferroelectrics. *Ferroelectrics* **76,** 241–267 (1987).
18. Kamba, S. *et al.* Dielectric dispersion of relaxor PLZT ceramics in the frequency range 20 Hz-100 THz. *J. Phys. Condens. Matter* **12,** 497–519 (2000).
19. Lunkenheimer, P. *et al.* Origin of apparent colossal dielectric constants. *Phys. Rev. B* **66,** 052105 (2002).
20. Austin, I. G. & Mott, N. F. Polarons in crystalline and non-crystalline materials. *Adv. Phys.* **18,** 41–103 (1969).
21. Callen, E. Optical absorption edge of magnetic semiconductors. *Phys. Rev. Lett.* **20,** 1045–1048 (1968).
22. Grimes, N. W. Off-centre ions in compounds with spinel structure. *Phil. Mag.* **26,** 1217–1226 (1972).
23. Ramirez, A. P. in *Handbook of Magnetic Materials* Vol. 13 (ed. Buschow, K. H. J.) 423–520 (Elsevier, Amsterdam, 2001).
24. Ramirez, A. P. Magic moments. *Nature* **421,** 483 (2003).
25. Mary, T., Evans, J. S. O., Vogt, T. & Sleight, A. W. Negative thermal expansion from 0.3 to 1050 K in ZrW_2O_8. *Science* **272,** 90–92 (1996).
26. Cao, D., Bridges, F., Kowach, G. R. & Ramirez, A. P. Frustrated soft modes and negative thermal expansion in ZrW_2O_8. *Phys. Rev. Lett.* **89,** 215902 (2002).
27. Knorr, K. & Loidl, A. Anomalous diffraction profiles of alkali-halide-alkali-cyanide mixed crystals. *Phys. Rev. Lett.* **57,** 460–462 (1986).
28. Höchli, U. T., Knorr, K. & Loidl, A. Orientational glasses. *Adv. Phys.* **39,** 405–615 (1990).
29. Lunkenheimer, P., Schneider, U., Brand, R. & Loidl, A. Glassy dynamics. *Contemp. Phys.* **41,** 15–36 (2000).

Acknowledgements This work was supported partly by the Deutsche Forschungsgemeinschaft via the Sonderforschungsbereich 484 and partly by the BMBF via VDI/EKM.

Competing interests statement The authors declare that they have no competing financial interests.

Correspondence and requests for materials should be addressed to P.L. (peter.lunkenheimer@physik.uni-augsburg.de).

Two-electron dissociation of single molecules by atomic manipulation at room temperature

P. A. Sloan* **& R. E. Palmer**

Nanoscale Physics Research Laboratory, School of Physics and Astronomy, The University of Birmingham, Edgbaston, Birmingham B15 2TT, UK

* Present address: Department of Chemistry, University of Toronto, 80 St George Street, Toronto, Ontario, M5S 3H6, Canada

Using the tip of a scanning tunnelling microscope (STM) to mechanically manipulate individual atoms and molecules on a surface is now a well established procedure[1,2]. Similarly, selective vibrational excitation of adsorbed molecules with an STM tip to induce motion or dissociation has been widely demonstrated[3,4]. Such experiments are usually performed on weakly bound atoms that need to be stabilized by operating at cryogenic temperatures. Analogous experiments at room temperature[5] are more difficult, because they require relatively strongly bound species that are not perturbed by random thermal fluctuations. But manipulation can still be achieved through electronic excitation of the atom or molecule by the electron current[6–11] tunnelling between STM tip and surface at relatively high bias voltages[10,11], typically 1–5 V. Here we use this approach to selectively dissociate chlorine atoms from individual oriented chlorobenzene molecules adsorbed on a Si(111)-7 × 7 surface. We map out the final destination of the chlorine daughter atoms, finding that their radial and angular distributions depend on the tunnelling current and hence excitation rate. In our system, one tunnelling electron has nominally sufficient energy to induce dissociation, yet the process requires two electrons. We explain these observations by a two-electron mechanism that couples vibrational excitation and dissociative electron attachment steps.

Figure 1 presents a sequence of STM images, acquired at room temperature and in ultrahigh vacuum, illustrating the dissociation of a single chlorobenzene molecule and the characterization of this event by careful STM imaging at different bias voltages. Figure 1a–d shows STM images obtained as the voltage applied to the Si(111)-7 × 7 surface is increased from +1 V to +4 V. The chlorobenzene molecule undergoing dissociation at +4 V is labelled α; it generates a chlorine atom bound to site β. γ and δ label chlorobenzene molecules that desorb at the same time. The experimental identification of the dissociation and desorption channels and of the dissociation fragments is based on the appearance of the relevant species in STM images as a function of the bias voltage[12], as illustrated in Fig. 1f–h. The desorption of molecules from sites γ and δ is apparent from the reappearance of the underlying silicon adatoms in Fig. 1g and h. The chlorine atom produced by single molecule dissociation appears as the bright feature at site β in